PROCEEDINGS OF SCIENCE

On the Reduction of the Error in the Calculation of Low Energy (<1GeV) Atmospheric Neutrino Flux

M. Honda*
Institute for Cosmic Ray Research, the University of Tokyo, 5-1-5 Kashiwa-no-ha,Kashiwa, Chiba 277-8582, Japan
E-mail: mhonda@icrr.u-tokyo.ac.jp

M. Sajjad Athar
Department of Physics, Aligarh Muslim University, Aligarh-202002, India
E-mail: sajathar@gmail.com

T. Kajita
Institute for Cosmic Ray Research, the University of Tokyo, 5-1-5 Kashiwa-no-ha,Kashiwa, Chiba 277-8582, Japan
E-mail: kajita@icrr.u-tokyo.ac.jp

K. Kasahara
Shibaura Institute of Technology, 307 Fukasaku, Minuma-ku, Saitama 337-8570, Japan
E-mail: kasahara@icrc.u-tokyo.ac.jp

S. Midorikawa
Faculty of Software and Information Technology, Aomori University, 2-3-1 Kobata, Aomori, Aomori 030-0943, Japan
E-mail: midori@aomori-u.ac.jp

Jun Nishimura
Institute of Space and Astronomical Science, JAXA, Sagamihara, Japan
E-mail: ANB05012@nifty.com

Using a semi-analytic formulation, we study the varations of the atmospheric neutrino and muon fluxes calculated with the variations of a hadronic interaction model. Considering the difference of the hadronic interaction model from the true one as variation of hadronic interaction model, we can estimate the the calculation error of the atmospheric neutrino flux by comparing of the atmospheric muon flux calculated and the observed one in a presition experiment. We find a relation between the reconstruction residual of the observed muon flux and the error of the atmospheric neutrino flux prediction. Then we studied the atmospheric muon flux at sevaral candidate of the observation site, Tsukuba (sea level), Mt. Norikura (2770m a.s.l.), Hanle India (4500m a.s.l.) , and Balloon altitude ($\sim$ 32km a.s.l.) near South Pole, to find a proper observation site for this study. We find the muon flux observed at high mountain is most useful to reduce the error of the atmospheric neutrino flux prediction.

36th International Cosmic Ray Conference -ICRC2019-
July 24th - August 1st, 2019
Madison, WI, U.S.A.

*Speaker.

© Copyright owned by the author(s) under the terms of the Creative Commons Attribution-NonCommercial-NoDerivatives 4.0 International License (CC BY-NC-ND 4.0).

PoS(ICRC2019)914

1. Introduction

Neutrino oscillation physics has now entered into precision era, For the atmospheric neutrino, precision experiments are also planned at INO [1], South Pole [2], HyperK [3], and DUNE [4], etc. To address some of the neutrino oscillation parameters, one requires accurate neutrino flux prediction in the $\lesssim 1$ GeV energy region. However, it is difficult to calculate the atmospheric neutrino flux below 1 GeV accurately. The major source of the uncertainty of the atmospheric neutrino flux calculation is in those of primary cosmic ray spectra and hadronic interactions. Fortunately, with the recent study of primary cosmic ray spectra by AMS02 and other precision measurements [5, 6, 7, 8], the uncertainty is reasonably reduced to a few %. On the other hand the uncertainty of hadronic interaction model is still large. It seems difficult to reduce the uncertainty to the required level using only the result of high energy experiment. This paper is an extension of the study in Ref.[9] to lower energies. We have had used the precision data of the muon flux to calibrate the hadronic interaction model. There were some preceding works on the same idea (for example, see the reference [10, 11]).

In this paper we use a semi-analytic formalism for the calculation of the atmospheric lepton flux, and study the variation of hadronic interaction model and the response of atmospheric leptons to that. Then establish a method to estimate the atmospheric neutrino flux prediction error from the atmospheric muon calculation error. For the above study we study the atmospheric muon flux at near Kamioka site (0 and 2770m a.s.l.), Hanle (India 4500m a.s.l.), and at balloon altitude (South Pole 32km a.s.l. by Balloon).

2. Semi-analytic formalism for atmospheric lepton calculation and variation of hadronic interaction model.

Let us consider a semi-analytic expression which projects the atmospheric lepton flux calculation process to the hadronic interaction "phase space" ; spanned by the momenta of cosmic ray originated projectile particle and of the meson which create the lepton in its decay (cascade). The expression may be written as;

$$\begin{aligned}\Phi_L^{obs}(p_L^{obs},x^{obs}) = \sum_{N^{proj}}\sum_{M^{born}}\int\int\Big[\int M2L(M^{born},p_M^{born},x^{int},\,L^{obs},p_L^{obs},x^{obs}) \\ \times H_{int}(N^{proj},p_N^{proj},x^{int},M^{born},p_M^{born}) \\ \times \sigma^{prod}(N^{proj},E^{proj})\cdot\rho_{air}(x^{int}) \\ \times \Phi_{proj}(N^{proj},p_N^{proj},x^{int})dx^{int}\Big]\, dp_M^{born}dp_N^{proj}, \qquad (2.1)\end{aligned}$$

where we have considered all the projectile and meson combinations, and $M2L(M,p_M^{born},x^{born},L^{obs},p_L^{obs},x^{obs})$ is the probability that a meson M^{born} with momentum p_M^{born} at x^{born} decays and result in the lepton L^{obs} with momentum p_L^{obs} at x_L^{obs}, without a hadronic interaction with air nuclei, $H_{int}(N^{proj},p_N^{proj},M^{born},p_M^{born})$ is the probability that a projectile particle N^{proj} with momentum p_N^{proj} interact with air nuclei and produce M^{born} meson with momentum p_M^{born}, $\sigma^{prod}(N^{proj},E^{proj})$ is the production cross section of N^{proj} particle and air nuclei, $\rho_{air}(x^{int})$ is the nucleus density of the air at x^{int}, and $\Phi_{proj}(N^{proj},p_N^{proj},x^{int})$ is the flux of cosmic ray originated N^{proj}-particle at x^{int} with momentum p_N^{proj}.

PoS(ICRC2019)914

We can make the pseudo analytic expression Eq. 2.1 to a practical one, and carry out an analytic calculation in a 1-dimensional calculation scheme. However, it is not easy to carry out such an analytic calculation in a 3-dimensional scheme, and we normally carry out the 3-dimensional Monte Carlo simulation to calculate the atmospheric lepton flux. Here we use Eq. 2.1 just to illustrate the study of the uncertainty of the hadronic interaction model.

It is convenient to rewrite Eq. 2.1 as,

$$\Phi_L^{obs}(p_L^{obs},x^{obs}) = \sum_{N^{proj}} \sum_{M^{born}} \int\int D(N^{proj},p_N^{proj},M^{born},p_M^{born},\ L^{obs},p_L^{obs},x^{obs})\ dp_M^{born} dp_N^{proj}\ , \quad (2.2)$$

where

$$\begin{aligned} D(N^{proj},p_N^{proj},M^{born},p_M^{born},\ L^{obs},p_L^{obs},x^{obs}) = \int & M2L(M^{born},p_M^{born},x^{int},\ L^{obs},p_L^{obs},x^{obs}) \\ & \times H_{int}(N^{proj},p_N^{proj},x^{int},M^{born},p_M^{born}) \\ & \times \sigma^{prod}(N^{proj},E^{proj}) \cdot \rho_{air}(x^{int}) \\ & \times \Phi_{proj}(N^{proj},p_N^{proj},x^{int})\ dx^{int}\ , \end{aligned} \quad (2.3)$$

As the atmospheric lepton flux is normally calculated with the Monte Carlo simulations, the D-function or integrand of Eq. 2.2 is also calculated with the Monte Carlo simulation. We tag all the particles appeared in the simulation, and record the momenta of the projectile particle and the meson when the meson creates the target lepton without any hadronic interaction. Then we study the (p_M^{born}, p_N^{proj}) point distribution in the hadronic interaction phase space.

The Monte Carlo simulation we use here is the same one which we have used for our prevopis calculation of atmospheric neutrino and atmospheric muon fluxes [12, 13]. We note that the full 3D Monte Carlo simulation for atmospheric neutrino need a long computation time, since it is an Earth size simulation for upward moving neutrinos. However, if we limit the calculation to the downward going neutrinos, it is completed far quickly. Therefore we consider here only the downward moving atmospheric neutrino and muon fluxes.

We show such an example in Fig. 1 as the scatter plot for the 1 GeV/c vertically downward moving muons at Tsukuba (sea level), and for 1 GeV vertically downward moving neutrino at

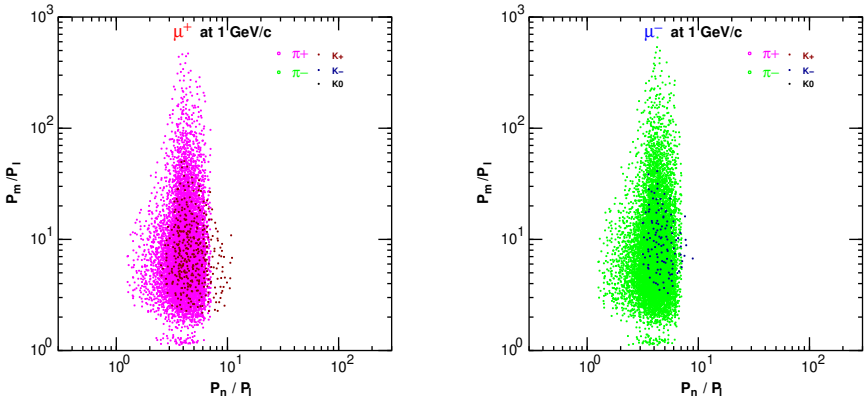

Figure 1: The distribution of projectile and meson momentum, which create 1 GeV/c downward moving atmospheric muon at Kamioka (sea level), in the (P_N, P_M) phase space.

PoS(ICRC2019)914

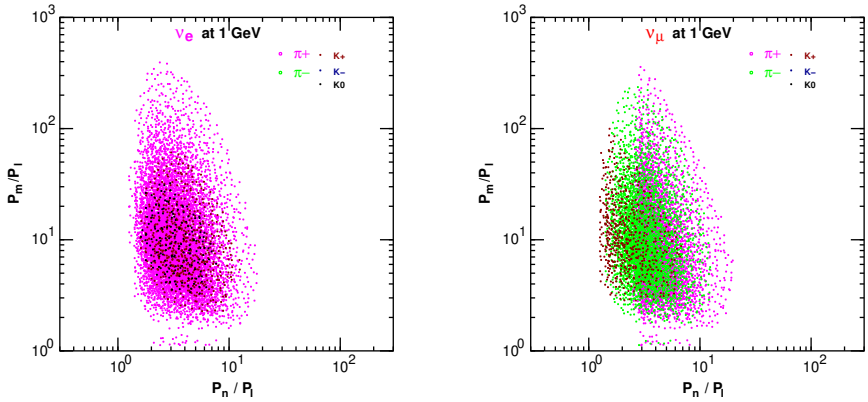

Figure 2: The distribution projectile and meson momenta, which create the 1 GeV vertically downward moving neutrino at Kamioka (sea level), in the (P_N, P_M) space.

Kamioka in Fig. 2, combining the different projectiles in the same figure.

We call the integrand or the D-function in Eq. 2.2 as the integral kernel of the atmospheric lepton flux. For each kind of lepton and it's mementum, we calculate the integral kernel for all the combination of projectile particle and secondary meson in the Monte Carlo simulation. We note the integral kernels of atmospheric muon and neutrino fluxes both have a large dependence on the moving direction. For the integral kernel of atmospheric muom flux, there is a large dependence on the observation site. if we limit the moving direction to the downward direction only. On the other hand, the integral kernel of atmospheric neutrino flux is not so sensitive to the observation site. We calculate the integral kernel of atmospheric neutrino flux for kamioka, and that of muon flux for several observation site, including Kamioka, and directions of the lepton motion.

If we assume that the projectile flux $\Phi_{proj}(N^{proj}, p_N^{proj}, x^{int})$ is not largely affected by the variation of the hadronic interactions, The effect of the variation of the hadronic interactions on the lepton flux can be studied using the formalism of the calculation of the atmospheric neutrino flux in the previous section. The lepton flux calculated by the variated interaction model may be written as;

$$\tilde{\Phi}_L^{obs}(p_L^{obs}, x^{obs}) = \sum_{N^{proj}} \sum_{M^{born}} \int\int D(N^{proj}, p_N^{proj}, M^{born}, p_M^{born}, L^{obs}, p_L^{obs}) \times \left(1 + \Delta_{int}(N^{proj}, M^{born}, p_N^{proj}, p_M^{born})\right) dp_M^{born} dp_N^{proj} . \quad (2.4)$$

We can use Eq. 2.4 to construct a variation of interaction model and the variation of atmospheric lepton fluxes and study it.

3. The interaction models with random number.

Variations of the hadronic interaction model with random number can be constructed with the help of the b-spline functions. We use the 3rd order b-spline function with constant knots separation which is represented as

$$B_\Delta^i(x) = b\left(\frac{x - i\cdot\Delta}{\Delta} - x_0\right) \quad (3.1)$$

PoS(ICRC2019)914

where

$$b(t) = \begin{cases} \frac{1}{6}(3|t|^3 - 6|t|^2 + 4) & (|t| \le 1) \\ -\frac{1}{6}(|t|-2)^3 & (1 \le |t| \le 2) \\ 0 & (|t| \ge 2) \quad , \end{cases} \tag{3.2}$$

Δ is the knots separation, and x_0 is for the shift less than Δ. The linear combination of 3rd order b-spline function (Eq. 3.1 and Eq. 3.2) is continuous up to 2nd order derivative, and is often used to connect the discrete data or to fit them. We can extend it to 2-dimensional bspline function as

$$B^{ij}_{\Delta}(x,y) = b\left(\frac{x - i\cdot\Delta}{\Delta} - x_0\right) b\left(\frac{y - j\cdot\Delta}{\Delta} - y_0\right) \quad , \tag{3.3}$$

Here, we took the same knots separation for x and y.

We may construct a variation function in Eq. 2.4 with these 2-dimensional b-spline function as

$$\Delta_{int}(N^{proj}, M^{born}, p_N^{proj}, p_M^{born}) = \delta \cdot \sum_i \sum_j R_N^{ij} \cdot B_{\Delta}^{ij}\left(\log_{10}(p_N^{proj},\ \log_{10}(p_M^{born})\right) \tag{3.4}$$

where $\{R_N^{ij}\}$ is the set of random numbers with normal distribution, and δ is a parameter to control the variation. Therefore, for each combination of the set of random numbers $\{R_N^{ij}\}$ and δ, we have a variation of the interaction model and the variation of flux as,

$$\begin{aligned} \Delta\Phi_L^{obs}(p_L^{obs}, x^{obs}) \equiv & \tilde{\Phi}_L^{obs}(p_L^{obs}, x^{obs}) - \Phi_L^{obs}(p_L^{obs}, x^{obs}) \\ = & \delta \sum_{N^{proj}} \sum_{M^{born}} \int\int D(N^{proj}, p_N^{proj}, M^{born}, p_M^{born},\ L^{obs}, p_L^{obs}) \\ & \times \sum_i \sum_j R_N^{ij} \cdot B_{\Delta}^{ij}\left(\log_{10}(p_N^{proj}),\ \log_{10}(p_M^{born})\right) dp_M^{born} dp_N^{proj} \ , \end{aligned} \tag{3.5}$$

As an application of the variation of the interaction model with random number, we study the correlation of atmospheric neutrino and atmospheric muon fluxes. let us define the correlation coefficient as,

$$\gamma(p_\nu^{obs}, x_\nu^{obs}; p_\mu^{obs}, x_\mu^{obs}) = \frac{\sum\left(\Delta\Phi_\nu(p_\nu^{obs}, x_\nu^{obs})\Delta\Phi_\mu(p_\mu^{obs}, x_\mu^{obs})\right)}{\sqrt{\sum\left(\Delta\Phi_\nu^k(p_\nu^{obs}, x_\nu^{obs})\right)^2 \sum\left(\Delta\Phi_\mu^k(p_\mu^{obs}, x_\mu^{obs})\right)^2}} \tag{3.6}$$

and study the correlation coefficient between muon and neutrino fluxes at each combination of muon momentum and neutrino energy. We show the muon momentum at maximum correlation coefficient for the neutrino flux as the function of neutrino energy for all combination of $(\nu_\mu, \bar{\nu}_\mu, \nu_e, \bar{\nu}_e)$ and (μ^+, μ^-), when it has non trivial maximum in Fig. 3. Also in the same figure, we have plot the muon momenta where the correlation coefficent of muon and neutrino fluxes decrease to 0.9 times of the maximum at each neutrino energy. Note the neutrino creation kinematic makes 2 type of correlations . One is for the direct π-decay (left panel), and the other is for the $\pi - \mu$ decay cascade (right panel).

PoS(ICRC2019)914

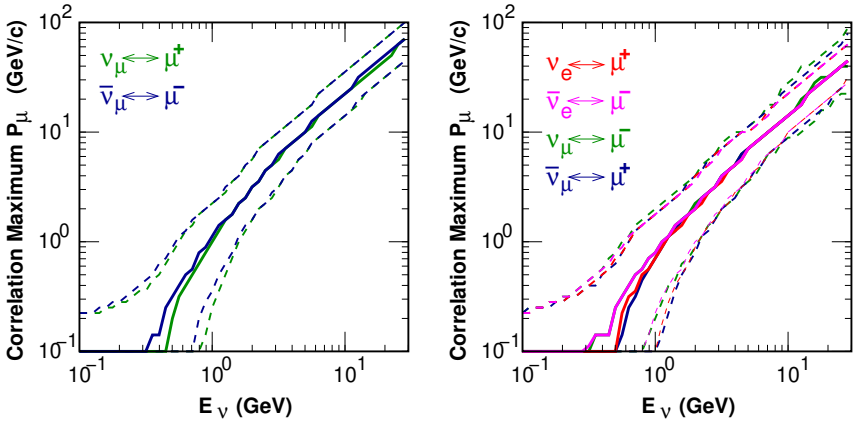

Figure 3: The momenta of atmospheric muon which show the maximum correlation and the 90% of that for the atmospheric neutrino as the funcion of the energy of neutrino energy. Left panel is for the neutrinos directly produced at the pion decay, and right panel is for the neutrinos produced at the decay of muon produced by the pion decay. We used the integral kernels of vertically downward moving atmospheric neutrinos and muons at Tsukuba or Kamioka (sea level)

4. Atmospheric neutrino flux variation with limited muon flux variation

Hereafter we just assume $\delta = 1$, but we consider the small variation of atmospheric muon flux by selecting the random numbers set $\{R_N^{ij}\}$, in Eq. 3.4 . Note, to take $\delta = 1$ is equivalent to assume 100 % uncertainty at each grid point of the hadronic interaction phase space for each meson $(\pi^{\pm}, K^{\pm,0})$ productions. To study the uncertainty of the a kind of atmospheric neutrino at a given neutrino energy, we consider the case that the muon variation is limited as $\Delta\phi_\mu/\phi_\mu < \varepsilon$ in muon momentum range where the correlation coefficient is larger than 0.9 times of the maximum, for the muons with non trivial correlation coefficient maximum. Then study the variation of the atmospheric neutrino flux. We plot the variation of $\Delta\Phi_\nu/\Phi_\nu$ at 1 GeV for ν_e in Fig.4 (left panel), taking $\varepsilon = 0.1$, 0.2, and 0.3. We find the distribution of $\Delta\Phi_\nu/\Phi_\nu$ shrinks as ε decreases.

Note, these distribution are well approximated with the normal distribution with the standard deviation of σ. Therefore the shrinkage is also expressed by a normal distribution with the standard deviation σ_{shrink} defined by the equation,

$$\frac{1}{\sigma_{shrink}^2} = \frac{1}{\sigma_\varepsilon^2} - \frac{1}{\sigma_\infty^2} \quad , \tag{4.1}$$

We assume a simple relation between σ_{shrink} and ε, such that

$$\sigma_{shrink} = \sqrt{\sigma_{res}^2 + (R\cdot\varepsilon)^2} \quad , \tag{4.2}$$

or we assumed that there is atmospheric neutrino variation related to atmospheric muon variation and independent of it. We fit σ_{shrink} with Eq. 4.2, and plot the fitting results In left panel of Fig. 4. We find the muon independent variation σ_{res} is around or less than 0.05 for the neutrino at 1 GeV.

Next we calculate the energy dependence of σ_{res} for all kind of vertically downward moving neutrino at Kamioka, using the integral kernel of vertically downward moving atmospheric muon at Kamioka (sea level) and plot it in the left panel of Fig. 5. and the integral kernel of vertically

PoS(ICRC2019)914

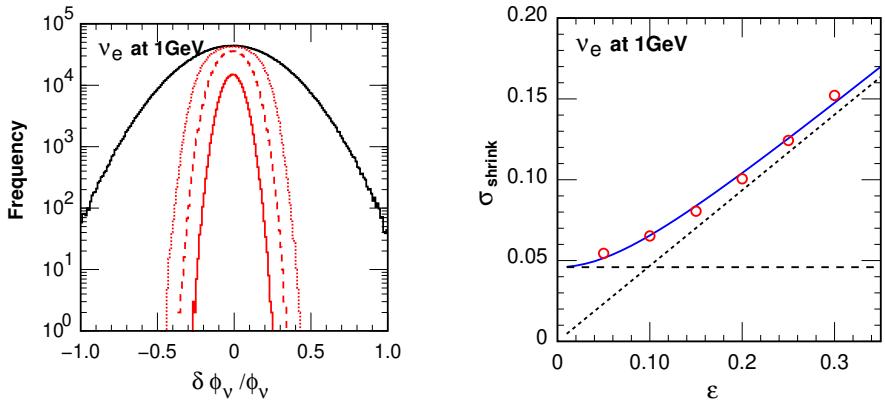

Figure 4: Left panel: the variation of ν_e flux. Outside wide solid line shows the distribution of $\Delta\phi_\nu/\phi_\nu$ constructed with Eq. 3.5 and $\delta = 1$ for 3000000 sets of normal random number assigned at each grid point. Inside lines show the muon variation suppressed distribution of $\Delta\phi_\nu/\phi_\nu$ with ε = 0.1, 0.2, 0.3 (narrow to wide). Right panel: $\sigma_{shirink}$ and fitting curve calculated with Eq. 4.2. Here, we used the integral kernels of vertically downward moving atmospheric neutrinos and muons at Kamioka (sea level) .

downward moving atmospheric muon at mountain altitude (Mt. Norikura, 2770m a.s.l.) in the right panel of Fig. 5.

We find the all the σ_{res} rise up for lower energy region below 1 GeV in the both panels of Fig. 5, but the rize is suppressed in the right panel. Thus, we can expect less increase of σ_{res} with the atmospheric muon flux observed higher altitude. In both panel, the variation of σ_{res} above 1 GeV is similar that there is a quicker rise of σ_{res} for ν_μ than other neutrinos. This is because the condition $\Delta\phi_\mu/\phi_\mu < \varepsilon$ dose not suppress the Kaon production uncertainty, and the contribution Kaon to ν_μ is larger than other neutrinos, and the condition Note, we have assumed 100 % uncertainty for the Kaon production.

We calculate σ_{res} using the integral kernel of the muon flux at much higher mountain (Hanle 4500m a.s.l. India) and at the Balloon altitude, and plot them in Fig. 6. We find in both the cases σ_{res} are almost the same as that for at sea level or lower mountain altitude, above 1 GeV. However, σ_{res} below 1 GeV is largely different by the observation altitude. Generally we can expect lower σ_{res} at higher mountain, but at the Balloon altitude it becomes even higher than that at the sea level. The Balloon altitude is considered too high, and the integral kernel for muon at this altitude and that for neutrino is observed at sea level is too different for this study.

Note, we can calculate σ_{res} for the horizontally moving neutrinos, using the integral kernel of vertically downward moving muon at sea level or at higher altitude. The rise of σ_{res} for lower energy is similar to vertically downward moving neutrino, but the rise for higher energy is smaller that of vertically downward moving neutrinos. This is because the contribution of Kaons to the atmospheric neutrino is still smaller than that for vertically downward moving neutrinos in this energy region.

5. Summary and Discussions

In order to improve the accuracy of the calculation of the low energy atmospheric neutrino flux, we have studied the response of atmospheric neutrino and atmospheric muon fluxes to the

PoS(ICRC2019)914

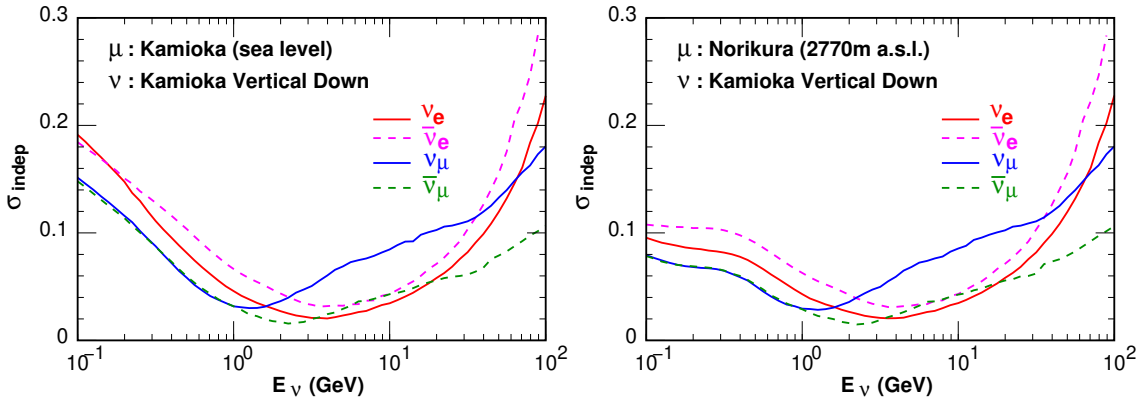

Figure 5: σ_{res} calculated by the fitting with Eq. 4.2 as the function of neutrino energy for all kind of neutrinos. Left panel is for the vertically downward moving neutrino with the integral kernel of muon flux at Kamioka (sea level). Right panel is the same as the left panel but with the integral kernel of muon flux at Mt. Norikura (2770m a.s.l.).

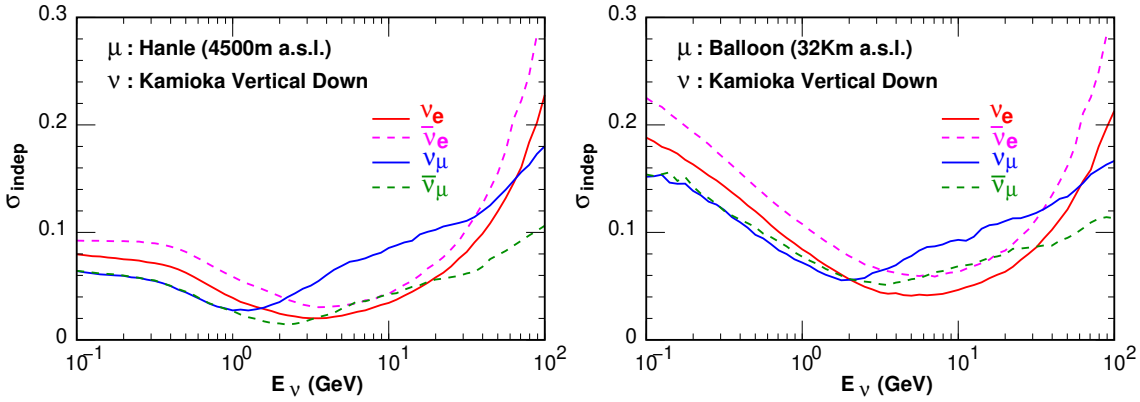

Figure 6: σ_{res} calculated by the fitting with Eq. 4.2 as the function of neutrino energy for all kind of neutrinos. Left panel is for the vertically downward moving neutrino with the integral kernel of muon flux at Hanle (4500m a.s.l.). Right panel is the same as the left panel but with the integral kernel of muon flux at Balloon altitude (32Km a.s.l.).

variation in the hadronic interaction model based on the semi-analytic formalism.

We construct a huge number of the random variation of the hadronic interaction model and calculate the atmospheric neutrino and muon fluxes. Then studied the variation of atmospheric neutrino flux when the variation of atmospheric muon flux is suppressed. We find that the variation of atmospheric neutrino flux is also suppressed, and the variation of atmospheric neutrino flux is statistically parametrized by the suppression degree of the atmospheric muon. This parameterization could be used to estimate the uncertainty of the atmospheric neutrino flux from the reconstruction residual of the observed atmospheric muon flux in a precise measurement.

We have had done a similar study in Ref. [9] using the muon fluxes observed by BESS detector at Tsukuba (sea level)[14], and at Mt. Norikura (2770m a.s.l.)[15]. The study of this paper could be applied to those observation, but with a caution for neutrino energy less than 1 GeV, since their lowest muon momenta observed were around 0.55 GeV/c, and are higher than what we have

PoS(ICRC2019)914

assumed here. However, this study agrees with the previous one for the neutrino energy above 1 GeV.

The atmospheric muon flux observation at higher mountain than Mt. Norikura (for example, Hanle India, 4500m a.s.l.) would give more stringent result for the atmospheric neutrino uncertainty, as the atmospheric neutrino independent component is smaller for the atmospheric muon flux observed at higher mountains. However, the muon flux at Balloon altitudes ($\sim$ 32 km a.s.l.) has a larger the atmospheric neutrino flux independent component, probably due to very high altitude.

Acknowledgments

We thank the ICRR of the University of Tokyo, especially for the use of the computer system.

References

[1] S. Ahmed et al. (ICAL), Pramana 88, 79 (2017), 1505.07380.

[2] M. G. Aartsen et al. (IceCube), J. Phys. G44, 054006 (2017), 1607.02671.

[3] K. Abe et al. (Hyper-Kamiokande) (2018), 1805.04163.

[4] R. Acciarri et al. (DUNE) (2016), 1601.05471.

[5] M. Aguilar et al. (AMS Collaboration), Phys. Rev. Lett. 114, 171103 (2015).

[6] M. Aguilar et al. (AMS), Phys. Rev. Lett. 115, 211101 (2015).

[7] O. Adriani et al., The Astrophysical Journal 765, 91 (2013).

[8] K. Abe et al., Adv. Space Res. 60, 806 (2017).

[9] T. Sanuki, M. Honda, T. Kajita, K. Kasahara, and S. Midorikawa, Phys. Rev. D75, 043005 (2007), astro-ph/0611201.

[10] D. H. Perkins, Astropart. Phys. 2, 249 (1994).

[11] D. H. Perkins, Nucl. Phys. B399, 3 (1993).

[12] M. Honda, T. Kajita, K. Kasahara, and S. Midorikawa, Phys. Rev. D83, 123001 (2011), 1102.2688.

[13] M. Honda, T. Kajita, K. Kasahara, and S. Midorikawa, Phys. Rev. D92, 023004 (2015), 1502.03916.

[14] S. Haino et al. (BESS), Phys. Lett. B594, 35 (2004).

[15] T. Sanuki et al., Phys. Lett. B541, 234 (2002), see also erratum [?].

[16] G. Battistoni, A. Ferrari, T. Montaruli, and P. R. Sala, Astropart. Phys. 19, 269 (2003).

PoS(ICRC2019)914